

FIRST PRINCIPLES STUDY OF ELASTIC AND THERMODYNAMIC PROPERTIES OF MgXSi (X = Mg, Sr)

¹Olayinka A.S., ²Nwankwo W. and ³Olayinka T.C.

¹Department of Physics, Edo University Iyamho

²Department of Computer Science, Edo University Iyamho.

³Department of Computer Science, Samuel Adegboyege University, Ogwa, Edo State

Abstract

In this paper, an application of the first principles investigation of elastic and thermal properties of MgXSi (X=Mg, Sr) compounds was conducted. The density functional theory (DFT) with pseudo-potential plane-waves approach using Projector Augmented Wave (PAW) method for the exchange and correlation potential was employed. Elastic constants and elastic compliances of MgXSi as well as the vibrational free energies, entropy, constant volume specific heat capacities were computed and presented. Our results show that elastic constants of Mg₂Si agree with previous theoretical results and compare favourably with experimental data. Elastic constants and compliances of MgSrSi are presented and discussed. Elastic constant, C₁₁ of 166.8GPa was recorded at the Debye temperature of 341.9K for Mg₂Si. At 300K, Constant Volume specific heat capacity, C_v for Mg₂Si and MgSrSi were measured to be 62.8 J/K/(N mol) and 70 J/K/(N mol) respectively.

Keywords: Elastic constants; first-principle; heat capacity; MgXSi; Elastic compliances.

1. Introduction

Desire for less toxic, naturally abundant and cost-effective materials has led to continuous investigations of Magnesium based alloys and compounds due to their potentials for use in several technological applications such as; thermoelectric, photo-voltaic, piezoelectric and infrared photonics. [1-3]. Mechanical alloy of Tin (Sn) into Magnesium silicide (Mg₂Si) have been reported to exhibits better comprehensive properties and thermoelectric properties than Mg₂Si. Difficulties in the experimental set up includes differences in temperatures of constituent's elements and contamination in material processing. Magnesium silicide is one of the silicides that is more prominent in solid state application because of its compatibility with Silicon, which is a based material for solid state devices and electronics. This material has high thermal stability as well as desirable oxidization resistance properties which makes fit as a green material for semiconductor applications. It is a semiconductor with narrow band gap, which has been used at a wavelength range of 1.2 to 1.8 micrometers as an infrared detector[4-6]. Doping and alloying have been used to enhance properties of semiconductors for optimum applications in optoelectronics and energy generations [7-8]. Elastic properties of the Mg₂Si structure under pressure have been reported by Zhang et al., their calculated elastic constants are stable at minimal pressure range of 0 to 7GPa under Born stability conditions. at low pressures [4]. Experimental measurement of the compressive-to-phase transformation characteristics of Mg₂Si at room temperature was reported by Hao et al. [10]. Some literatures only report elastic constants and young modulus without leaving out other elastic properties in their work. In this paper, we present a first-principles calculations of elastic properties and some thermodynamic properties of MgXSi (X = Mg, Sr) in antifluorite face-centered cubic (FCC) structure. The elastic constants, elastic compliances and specific heat capacities at constant volume, C_v and the Debye temperatures θ_D of Mg₂Si and MgSrSi are computed and discussed. The results are compared with available experimental and theoretical results.

2. The Calculation Model and Method

The computation is based on the density functional theory (DFT) [11] using the Projected Augmented Wave (PAW) PBE functional which defines the exchange-correction energy. First-principles computations were carried in this work. The PBE-

Correspondence Author: Olayinka A.S., Email: akinola.olayinka@edouniversity.edu.ng, Tel: +2348062447411

Transactions of the Nigerian Association of Mathematical Physics Volume 13, (October - December, 2020), 9 –20

PAW pseudo-potential were used to describe the ionic core and valence electrons interactions. The pseudo-potentials used in materials modeling are Mg.pbe-spn-kjpaw_psl.1.0.0.UPF, Si.pbe-n-kjpaw_psl.1.0.0.UPF and Sr.pbe-spn-kjpaw_psl.1.0.0.UPF with configurations ([Ne] 3s2.0 3p0), ([Ne] 3s2 3p2 3d-1) and ([Kr] 5s2 5p0 4d-1) for Magnesium, Silicon and Strontium respectively. Brillouin zone sampling was performed by using the Monkhorst–Pack scheme [12] with a k-point grid of 8 x 8 x 8. Geometry optimization was considered to be performed when all components of all forces are smaller than 0.1 micro Ry. The plane wave cut-off energy was relaxed to 90 Ry. Relaxation of the atomic structures were carried out using the Broyden-Fletcher-Goldfarb-Shanno method [13]. All computations were carried out with thermo_pw [14] implementation on the Quantum Espresso (QE) code [15-16]. Elastic properties computed were further post processed and analysed using the ELATE code [17].

3 Results and Discussion

Results base on the computations are presented in this section for thermodynamical and elastic properties. The results are discussed and compared with other results from theory and experiments.

3.2 Thermodynamic Properties

The Helmholtz free energy within the quasi-harmonic approximation (QHA) which is fundamental to computing thermodynamical properties is given as [9,18, 19]

$$F(V, T) = U_{stat}(V) + k_B T \sum_{q\lambda} \ln \left(2 \sinh \left[\frac{\hbar \omega_{q\lambda}(V)}{2k_B T} \right] \right) + F_{el}(V, T) \quad (1)$$

where $U_{stat}(V)$ is the static internal energy at volume V and $k_B T \sum_{q\lambda} \ln \left(2 \sinh \left[\frac{\hbar \omega_{q\lambda}(V)}{2k_B T} \right] \right) + F_{el}(V, T)$ represent the vibrational free energy. \hbar is the reduced Planck constant, and $\hbar \omega_{q\lambda}(V)$ is the frequency of the phonon with wave vector q and polarization λ , evaluated at constant volume V . $F_{el}(V, T)$ is the thermal electronic contribution to free energy. Usually, it is assumed that the electronic contribution to total free energy can be negligible. The vibrational specific heat C_V at constant volume in the is given as

$$C_V^{vib} = \sum_{q\lambda} k_B \left(\frac{\hbar \omega_{q\lambda}(V)}{2k_B T} \right)^2 \text{cosh}^2 \left(\frac{\hbar \omega_{q\lambda}(V)}{2k_B T} \right) \quad (2)$$

The electronic specific heat can be obtained from

$$C_V^{el} = T \left(\frac{\partial S_{el}}{\partial T} \right)_V \quad (3)$$

and the total specific heat at constant volume is then $C_V = C_V^{ph} + C_V^{el}$. The specific heat at a constant pressure, C_p , is different from the specific heat at a constant volume, C_V due to anharmonicity. C_p goes to a constant which is given by classical equipartition law: $C_V = 3Nk_B$ where N is the number of atoms in the system and k_B is the Boltzmann's constant. The knowledge of heat capacity of a substance provides crucial information on its vibrational properties and applications [18].

The heat capacity at constant volume, C_V inclines towards the Petit and Dulong boundary at higher temperature, C_V is proportional to T^3 [9,20]. The volume thermal expansion coefficient is given as

$$\alpha(T) = \frac{1}{V} \left(\frac{\partial V}{\partial T} \right)_P \quad (4)$$

while the linear thermal expansion is given as [21]

$$\epsilon(T) = \left(\frac{a(T) - a(T_c)}{a(T_c)} \right) \quad (5)$$

where $a(T_c)$ is the equilibrium lattice constant and $a(T) = [V(T)]^{1/3}$ at $T_c = 300K$.

Vibrational contribution to the entropy of the system is given as [9]

$$S_{vib} = -k_B \sum_{q\lambda} \left[\ln \left(2 \sinh \frac{\hbar \omega_{q\lambda}(V)}{2k_B T} \right) - \frac{\hbar \omega_{q\lambda}(V)}{2k_B T} \coth \left(\frac{\hbar \omega_{q\lambda}(V)}{2k_B T} \right) \right] \quad (6)$$

Insight to heat capacity of a materials is helpful in understanding the vibrational properties of materials as well as their area of applications. The temperature, T dependent thermodynamic properties for $MgXSi$ ($X = Mg, Sr$) computed are presented in Figures 1 – 4. The figures show the thermodynamics properties for the two variant materials; Mg_2Si and $MgSrSi$ computed at temperature range of 0 to 800K. Figure 1 shows the Debye Vibrational Energy as a function of Temperature for Mg_2Si and $MgSrSi$. At 0 K, the Debye Vibrational Energies of 15.8 kJ/(N mol) and 10.0 kJ/(N mol) were measured while at the maximum temperature of 800 K, 61.8 kJ/(N mol) and 60 kJ/(N mol) were measured respectively for Mg_2Si and $MgSrSi$. Calculated values for Vibrational energies at 300K for Mg_2Si and $MgSrSi$ are 26.7 kJ/(N mol) and 23.5 kJ/(N mol) respectively. In figure 2, the computed Vibrational Free Energy if presented as function of Temperature. At temperatures 0K, 300K and 800K, the measured vibrational free energies are 15.8 kJ/(N mol), -0.9 kJ/(N mol) and -39.5 kJ/(N mol) for Mg_2Si and 10 kJ/(N mol), -4.9 kJ/(N mol) and -70.1 kJ/(N mol) for $MgSrSi$.

Figure 3 shows the entropy computed for Mg_2Si and $MgSrSi$ variants, the entropy for the two variants rises gradually from

around 27K for MgSrSi and 45K for Mg₂Si. The entropies of Mg₂Si peaked at 124.1 J/K/(N mol) while that of MgSrSi reached its peak at 164 J/K/(N mol) at the same temperature of 800K. At 300K, MgSrSi has better entropy values of 90.2 J/K/(N mol) as against 57.1 J/K/(N mol) for Mg₂Si at the same temperature. Entropy, which is a quantitative measure of disorder or randomness within a system is an important property in thermodynamics of material. in a system.

Constant Volume specific heat capacity, C_v of Mg₂Si and MgSrSi computed as a function of temperature is presented in figure 4, at low temperature, C_v obeys T^3 law. Specific heat capacity was zero for Mg₂Si and MgSrSi until they approached 26K and 20K respectively. Computed C_v for Mg₂Si and MgSrSi for at 300K is 62.8 J/K/(N mol) and 70 J/K/(N mol).

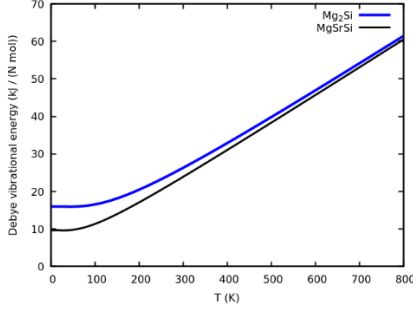


Figure 1: Debye Vibrational Energy for MgXSi (X=Mg, Sr).

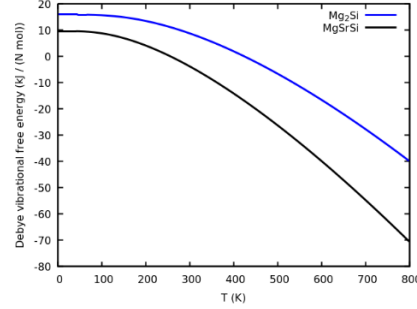


Figure 2: Debye Vibrational Free Energy for MgXSi (X=Mg, Sr).

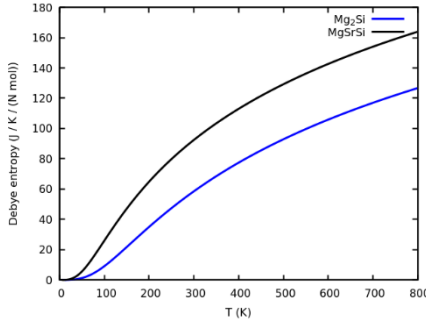


Figure 3: Calculated Entropy for MgXSi (X=Mg, Sr).

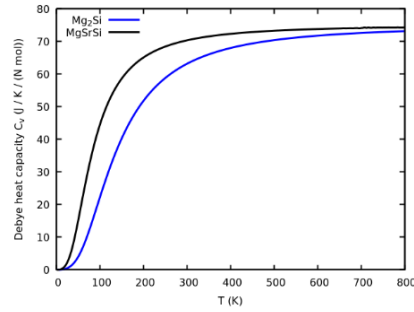


Figure 4: Calculated Heat Capacity for MgXSi (X=Mg, Sr).

3.2 Elastic Properties

For small deformation, each component of the stress tensor, σ is directly proportional the strain tensor, ϵ and vice versa as given below [22].

$$\sigma_{ij} = c_{ijkl}\epsilon_{kl} \tag{7}$$

$$\epsilon_{ij} = s_{ijkl}\sigma_{kl} \tag{8}$$

where i, j, k and l could be 1, 2, or 3. c_{ijkl} represents the components of elasticity tensor while s_{ijkl} represents the components of the elastic compliance tensor. The equation presents a fourth order tensor with $3^4 = 81$ independent components. These components are reduced to 36 components since $\sigma_{ij} = \sigma_{ji}$ and $\epsilon_{ij} = \epsilon_{ji}$. Since deformation process is considered to be reversible, the symmetry may be applied to the elasticity ($c_{ijkl} = c_{klij}$ and compliances $s_{ijkl} = s_{klij}$) tensors, thereby reducing the number of independent components to 21. Elastic constants and compliance are given as c and s , as shown in cartesian notation.

$$\begin{aligned} \sigma_{11} &= c_{11}\epsilon_{11} + c_{12}\epsilon_{22} + c_{13}\epsilon_{33} + c_{14}\epsilon_{23} + c_{15}\epsilon_{31} + c_{16}\epsilon_{12} \\ \sigma_{22} &= c_{21}\epsilon_{11} + c_{22}\epsilon_{22} + c_{23}\epsilon_{33} + c_{24}\epsilon_{23} + c_{25}\epsilon_{31} + c_{26}\epsilon_{12} \\ \sigma_{33} &= c_{31}\epsilon_{11} + c_{32}\epsilon_{22} + c_{33}\epsilon_{33} + c_{34}\epsilon_{23} + c_{35}\epsilon_{31} + c_{36}\epsilon_{12} \\ \sigma_{23} &= c_{41}\epsilon_{11} + c_{42}\epsilon_{22} + c_{43}\epsilon_{33} + c_{44}\epsilon_{23} + c_{45}\epsilon_{31} + c_{46}\epsilon_{12} \\ \sigma_{31} &= c_{51}\epsilon_{11} + c_{52}\epsilon_{22} + c_{53}\epsilon_{33} + c_{54}\epsilon_{23} + c_{55}\epsilon_{31} + c_{56}\epsilon_{12} \\ \sigma_{12} &= c_{61}\epsilon_{11} + c_{62}\epsilon_{22} + c_{63}\epsilon_{33} + c_{64}\epsilon_{23} + c_{65}\epsilon_{31} + c_{66}\epsilon_{12} \end{aligned} \tag{9}$$

$$\begin{aligned} \epsilon_{22} &= s_{21}\sigma_{11} + s_{22}\sigma_{22} + s_{23}\sigma_{33} + s_{24}\sigma_{23} + s_{25}\sigma_{31} + s_{26}\sigma_{12} \\ \epsilon_{33} &= s_{31}\sigma_{11} + s_{32}\sigma_{22} + s_{33}\sigma_{33} + s_{34}\sigma_{23} + s_{35}\sigma_{31} + s_{36}\sigma_{12} \\ \epsilon_{23} &= s_{41}\sigma_{11} + s_{42}\sigma_{22} + s_{43}\sigma_{33} + s_{44}\sigma_{23} + s_{45}\sigma_{31} + s_{46}\sigma_{12} \\ \epsilon_{31} &= s_{51}\sigma_{11} + s_{52}\sigma_{22} + s_{53}\sigma_{33} + s_{54}\sigma_{23} + s_{55}\sigma_{31} + s_{56}\sigma_{12} \\ \epsilon_{12} &= s_{61}\sigma_{11} + s_{62}\sigma_{22} + s_{63}\sigma_{33} + s_{64}\sigma_{23} + s_{65}\sigma_{31} + s_{66}\sigma_{12} \end{aligned} \tag{10}$$

The elastic constants, c and compliances, s are given in matrices form which shows inversion between elastic constants c and the compliances s ;

$$\begin{pmatrix} c_{11} & c_{12} & c_{13} & c_{14} & c_{15} & c_{16} \\ c_{12} & c_{22} & c_{23} & c_{24} & c_{25} & c_{26} \\ c_{13} & c_{23} & c_{33} & c_{34} & c_{35} & c_{36} \\ c_{14} & c_{24} & c_{34} & c_{44} & c_{45} & c_{46} \\ c_{15} & c_{25} & c_{35} & c_{45} & c_{55} & c_{56} \\ c_{16} & c_{26} & c_{36} & c_{46} & c_{56} & c_{66} \end{pmatrix} \text{ and } \begin{pmatrix} s_{11} & s_{12} & s_{13} & s_{14} & s_{15} & s_{16} \\ s_{12} & s_{22} & s_{23} & s_{24} & s_{25} & s_{26} \\ s_{13} & s_{23} & s_{33} & s_{34} & s_{35} & s_{36} \\ s_{14} & s_{24} & s_{34} & s_{44} & s_{45} & s_{46} \\ s_{15} & s_{25} & s_{35} & s_{45} & s_{55} & s_{56} \\ s_{16} & s_{26} & s_{36} & s_{46} & s_{56} & s_{66} \end{pmatrix} \tag{11}$$

Table 1 presents the elastic properties of computed for Mg_2Si and $MgSrSi$ in comparison with experimental data and other theoretical results. Computed lattice parameter for Mg_2Si compares favourably with experimental lattice constant of 0.6338nm as well as other theoretical results. Computed elastic constant, C_{11} is 116.0 GPa which compares well with other theoretical results. Percentage error of computed elastic constant and the experimental work is around 7.9%. Computed elastic constant for $MgSrSi$ is 166.8GPa which is higher than that the based material Mg_2Si . Resistance of materials to elastic deformation under load is measured as Young’s Modulus. Stiff materials have higher Young’s modulus than flexible materials. The computed Young’s modulus for Mg_2Si is higher than that of $MgSrSi$, thereby making a $MgSrSi$ a more flexible material than Mg_2Si . Computed compliances for Mg_2Si and $MgSrSi$ is presented in table 2. Further post processing and analysis of the stiffness matrix for Mg_2Si and $MgSrSi$ as shown in Table 3 using the online platform for Elastic tensor analysis called ELATE [26]. Average properties, Eigenvalues of the stiffness matrix and Variations of the elastic moduli for Mg_2Si and $MgSrSi$ are presented in tables 4 – 6 based on post processing done with ELATE. The two-dimensional (2D) and three-dimensional (3D) projections of Spatial dependence of Young’s Modulusfor Mg_2Si and $MgSrSi$ are presented in figure 5. The figure shows clear distinction in the projections for Mg_2Si and $MgSrSi$ both in 2D and 3D projections. Figure 6 shows the 2D and 3D projections of Spatial dependence of linear compressibility for Mg_2Si and $MgSrSi$. 2D and 3D Projection of Spatial dependence of shear modulus are presented in figure 7 for Mg_2Si and $MgSrSi$ while the same is presented for Spatial dependence of Poisson’s ratio in figure 8.

Table 1: Computed elastic properties for Mg_2Si and $MgSrSi$ in comparison with other results.

Properties	Mg_2Si					$MgSrSi$
	This Work	Experiment		Theoretical Work		This Work
		[23]	[24]	[1]	[25]	
Lattice Constant (nm)	0.6341	0.6338	-	0.676	0.6378	0.6361
C_{11} (GPa)	116.0	126	-	118.82	113.5	166.8
C_{12} (GPa)	22.6	26	-	22.27	22.8	67.2
C_{44} (GPa)	45.0	48.5	-	44.96	43.2	20.9
$S = (C_{11}-C_{12})/2C_{44}$	1.04	1.03	-	1.07	1.05	2.38
Bulk Modulus B (GPa)	53.7	59	-	54.45	53.1	100.3
Young’s Modulus E(GPa)	106.7	-	116.9	111.79	-	81.5
shear modulus G(GPa)	45.6	-	48.92	46.25	-	29.9
Poisson ratio ν	0.17	-	0.195	0.15	-	0.36
Average Debye sound velocity (m/s)	5287.752	-	-	-	-	3192.67
Debye temperature (K)	566.3	-	583	-	-	341.9

Table 2: Computed compliances for Mg_2Si and $MgSrSi$.

Properties	Mg_2Si	$MgSrSi$
S_{11} (1/Mbar)	0.92	0.77
S_{12} (1/Mbar)	-0.15	-0.22
S_{44} (1/Mbar)	2.22	4.77

Table 3: Stiffness matrix (GPa) for Mg₂Si and MgSrSi

Input to ELATE (GPa)					
Mg₂Si					
115.96	22.589	22.589	0	0	0
22.589	115.96	22.589	0	0	0
22.589	22.589	115.96	0	0	0
0	0	0	44.932	0	0
0	0	0	0	44.932	0
0	0	0	0	0	44.932
MgSrSi					
166.78	67.163	67.163	0	0	0
67.163	166.78	67.163	0	0	0
67.163	67.163	166.78	0	0	0
0	0	0	20.95	0	0
0	0	0	0	20.95	0
0	0	0	0	0	20.95

Table 4: Average properties

Averaging scheme	Bulk modulus	Young's modulus	Shear modulus	Poisson's ratio
Mg₂Si				
Voigt	$K_V = 53.714$ GPa	$E_V = 106.69$ GPa	$G_V = 45.634$ GPa	$\nu_V = 0.16896$
Reuss	$K_R = 53.714$ GPa	$E_R = 106.66$ GPa	$G_R = 45.618$ GPa	$\nu_R = 0.16905$
Hill	$K_H = 53.714$ GPa	$E_H = 106.67$ GPa	$G_H = 45.626$ GPa	$\nu_H = 0.169$
MgSrSi				
Voigt	$K_V = 100.37$ GPa	$E_V = 87.986$ GPa	$G_V = 32.494$ GPa	$\nu_V = 0.3539$
Reuss	$K_R = 100.37$ GPa	$E_R = 75.017$ GPa	$G_R = 27.27$ GPa	$\nu_R = 0.37543$
Hill	$K_H = 100.37$ GPa	$E_H = 81.552$ GPa	$G_H = 29.882$ GPa	$\nu_H = 0.36458$

Table 5: Eigenvalues of the stiffness matrix

λ_1	λ_2	λ_3	λ_4	λ_5	λ_6
Mg₂Si					
44.932 GPa	44.932 GPa	44.932 GPa	93.376 GPa	93.376 GPa	161.14 GPa
MgSrSi					
20.95 GPa	20.95 GPa	20.95 GPa	99.617 GPa	99.617 GPa	301.11 GPa

Table 6: Variations of the elastic moduli

	Young's modulus		Linear compressibility		Shear modulus		Poisson's ratio		
	E_{min}	E_{max}	β_{min}	β_{max}	G_{min}	G_{max}	ν_{min}	ν_{max}	
Mg₂Si									
Value	105.41 GPa	108.6 GPa	6.2057 TPa^{-1}	6.2057 TPa^{-1}	44.932 GPa	46.688 GPa	0.15941	0.18163	Value
Anisotropy	1.03		1.0000		1.039		1.1394		Anisotropy
Axis	0.5774 0.5774 0.5773	0.0000 0.0000 1.0000	0.0000 0.0000 1.0000	0.5000 0.0000 0.8660	0.0000 0.0000 1.0000	0.7071 -0.0002 0.7071	0.7071 0.0000 0.7071	-0.7071 -0.0000 -0.7071	Axis
					0.9397 0.3420 -0.0000	0.7071 -0.0006 -0.7071	0.0000 1.0000 -0.0000	-0.7071 0.0002 -0.7071	Second axis
MgSrSi									
Value	58.762 GPa	128.22 GPa	3.3211 TPa^{-1}	3.3211 TPa^{-1}	20.95 GPa	49.809 GPa	0.15219	0.62209	Value
Anisotropy	2.182		1.0000		2.377		4.0877		Anisotropy
Axis	0.5774 0.5773 -0.5774	0.0000 0.0000 1.0000	0.9659 0.0000 0.2588	-0.5624 0.7330 0.3827	0.0000 0.0000 1.0000	0.7071 -0.0003 0.7071	0.7071 -0.0002 -0.7071	-0.7071 -0.0002 -0.7071	Axis
					1.0000 0.0002 -0.0000	0.7071 -0.0005 -0.7071	0.0002 1.0000 -0.0002	0.7071 -0.0005 -0.7071	Second axis

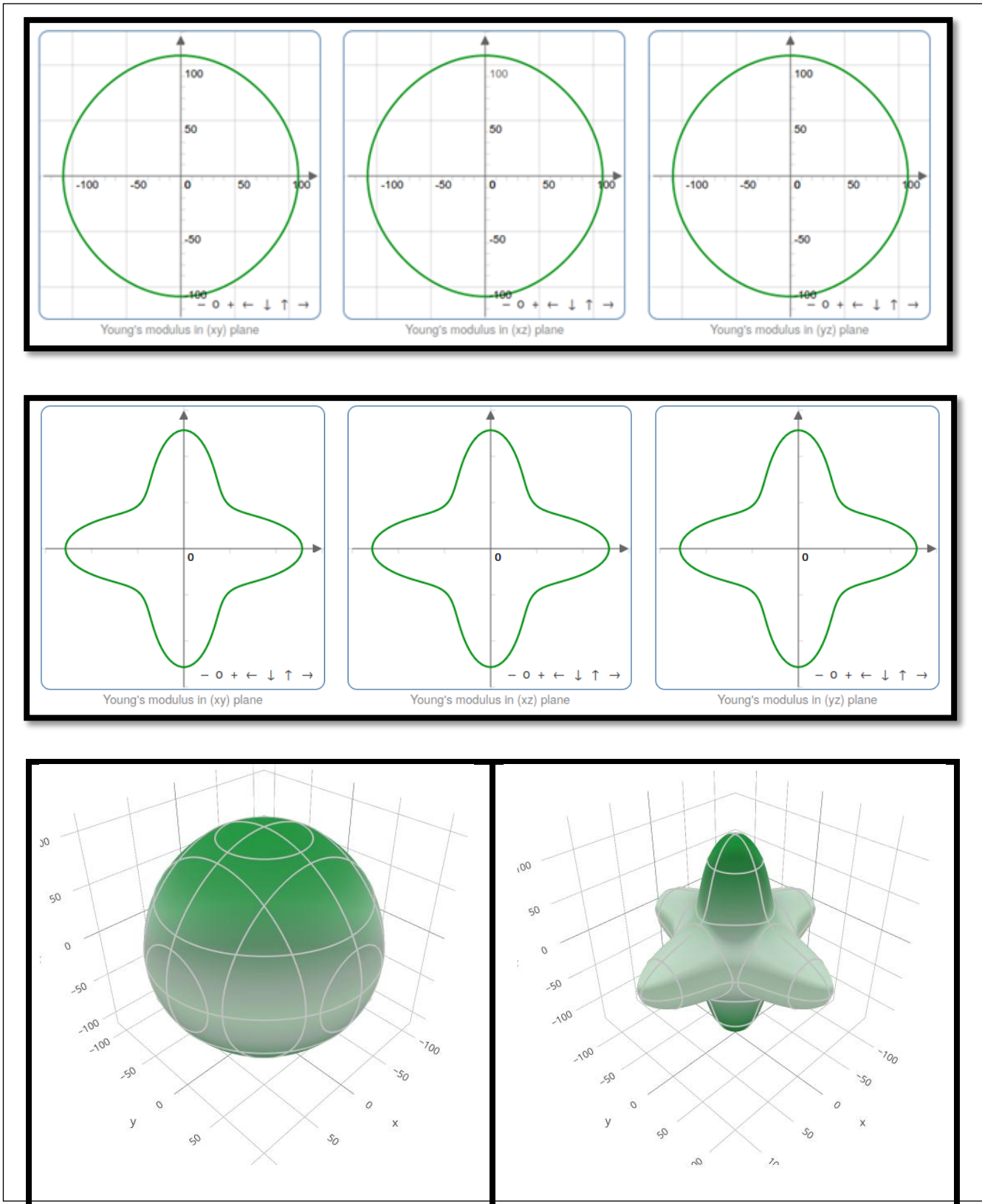


Figure 5: 2D and 3D Projection of Spatial dependence of Young's Modulus for Mg_2Si and $MgSrSi$

Transactions of the Nigerian Association of Mathematical Physics Volume 13, (October - December, 2020), 9 –20

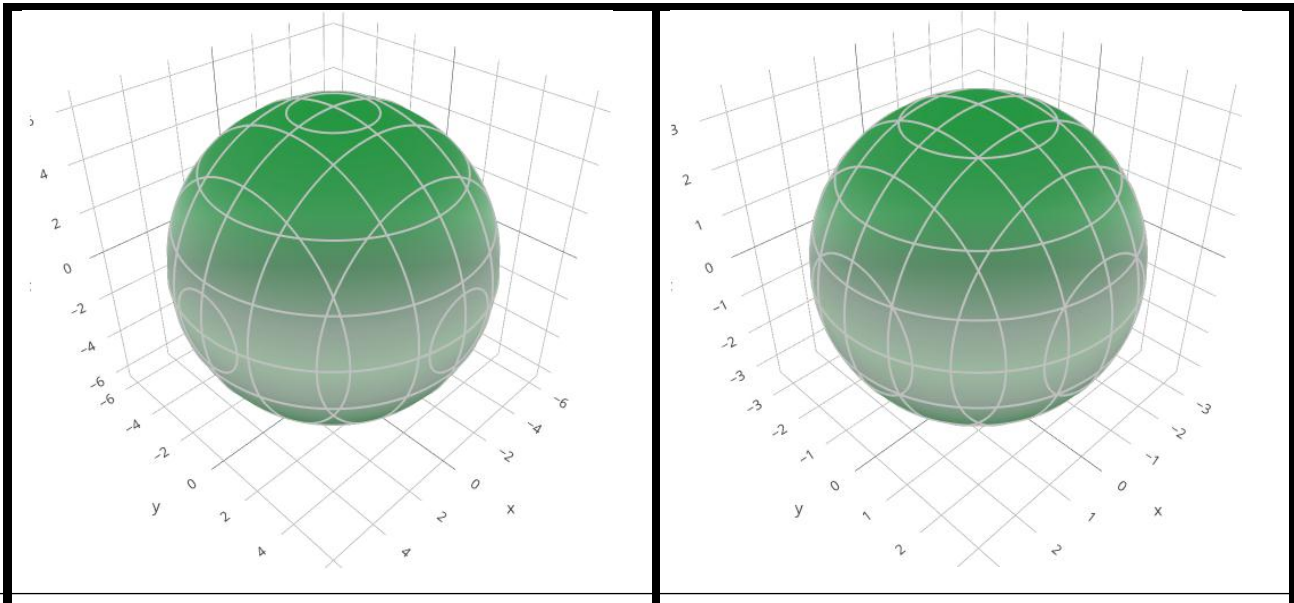
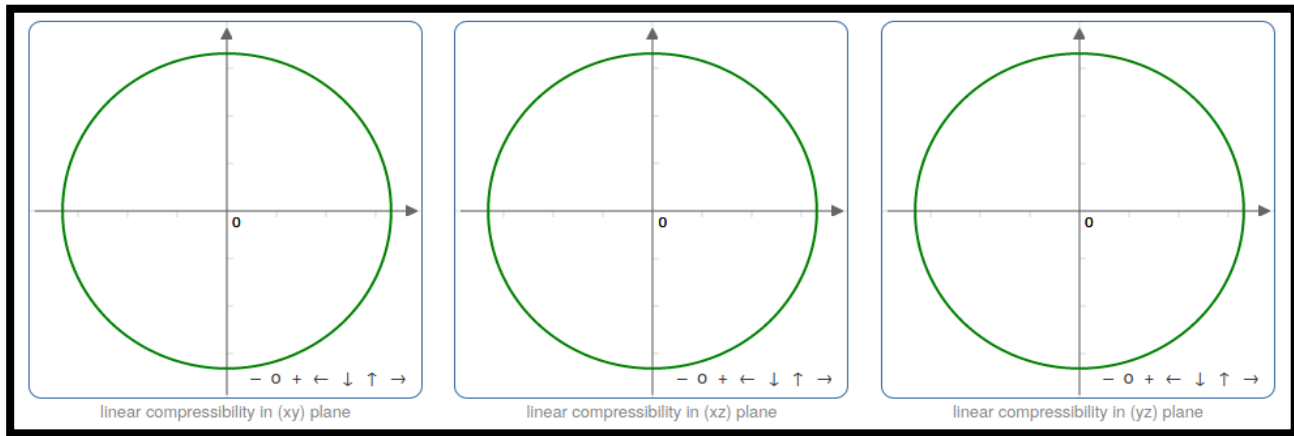
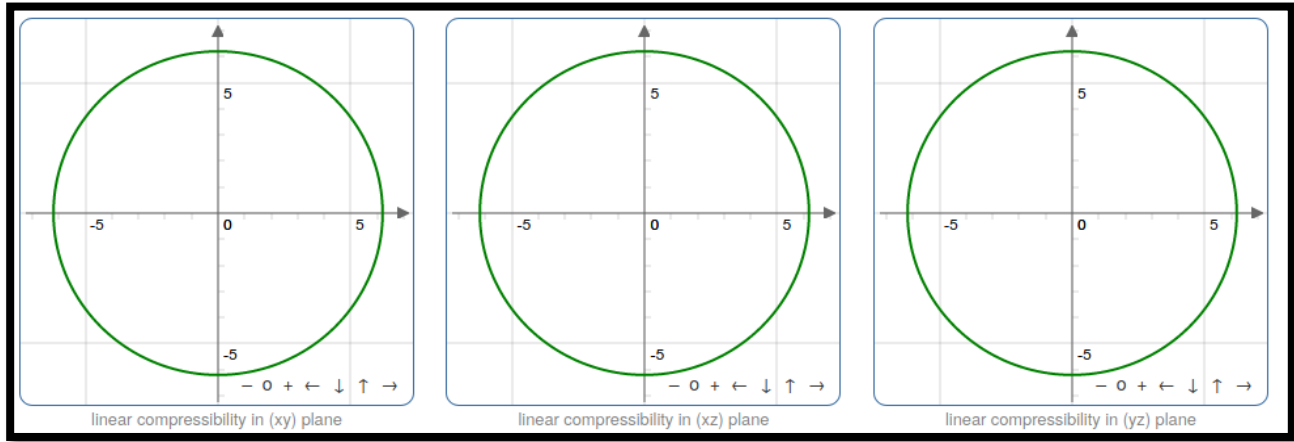


Figure 6: 2D and 3D Projection of Spatial dependence of linear compressibility for Mg_2Si and $MgSrSi$

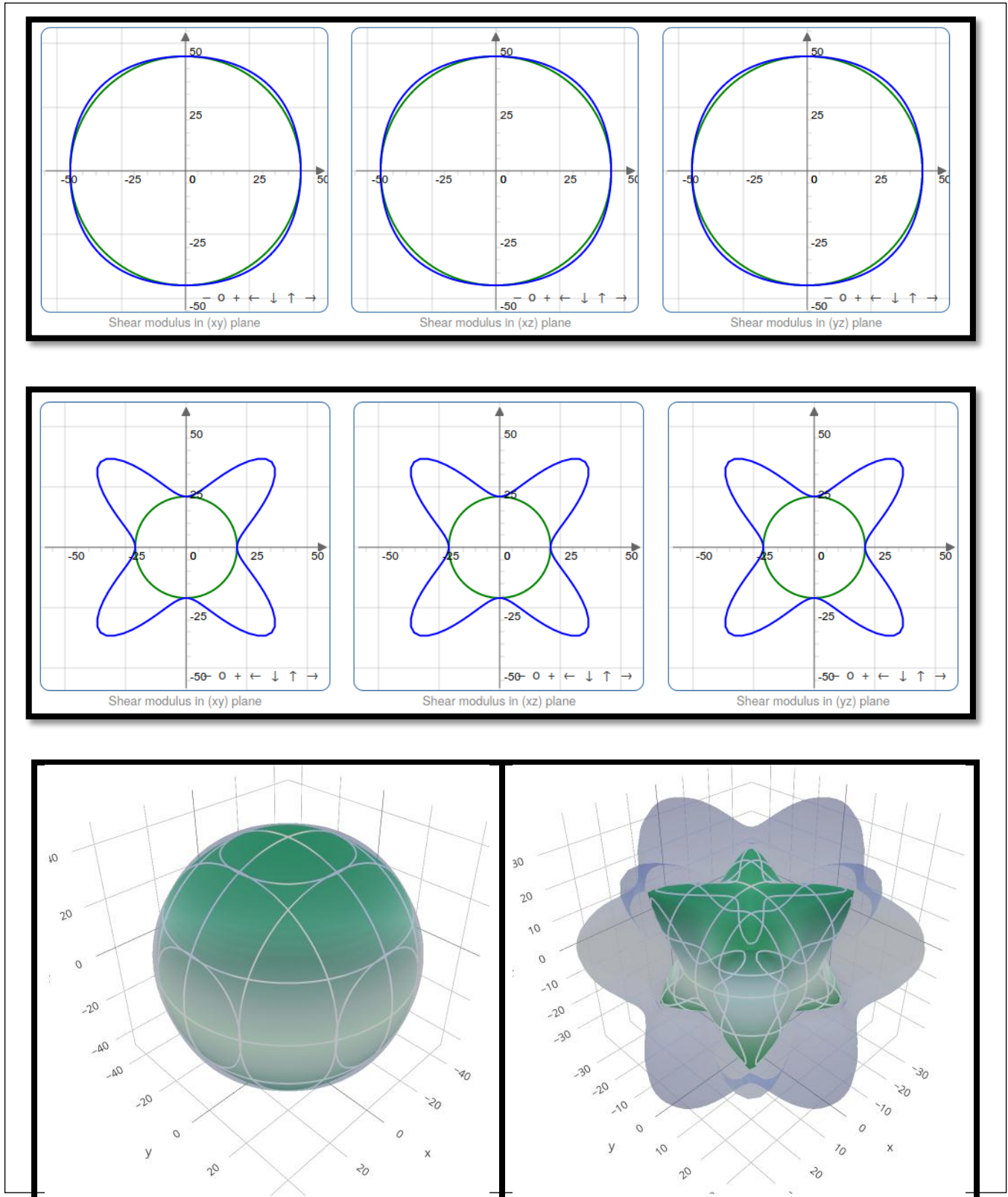


Figure 7: 2D and 3D Projection of Spatial dependence of shear modulus for MgSi and MgSiSi
Transactions of the Nigerian Association of Mathematical Physics Volume 13, (October - December, 2020), 9 –20

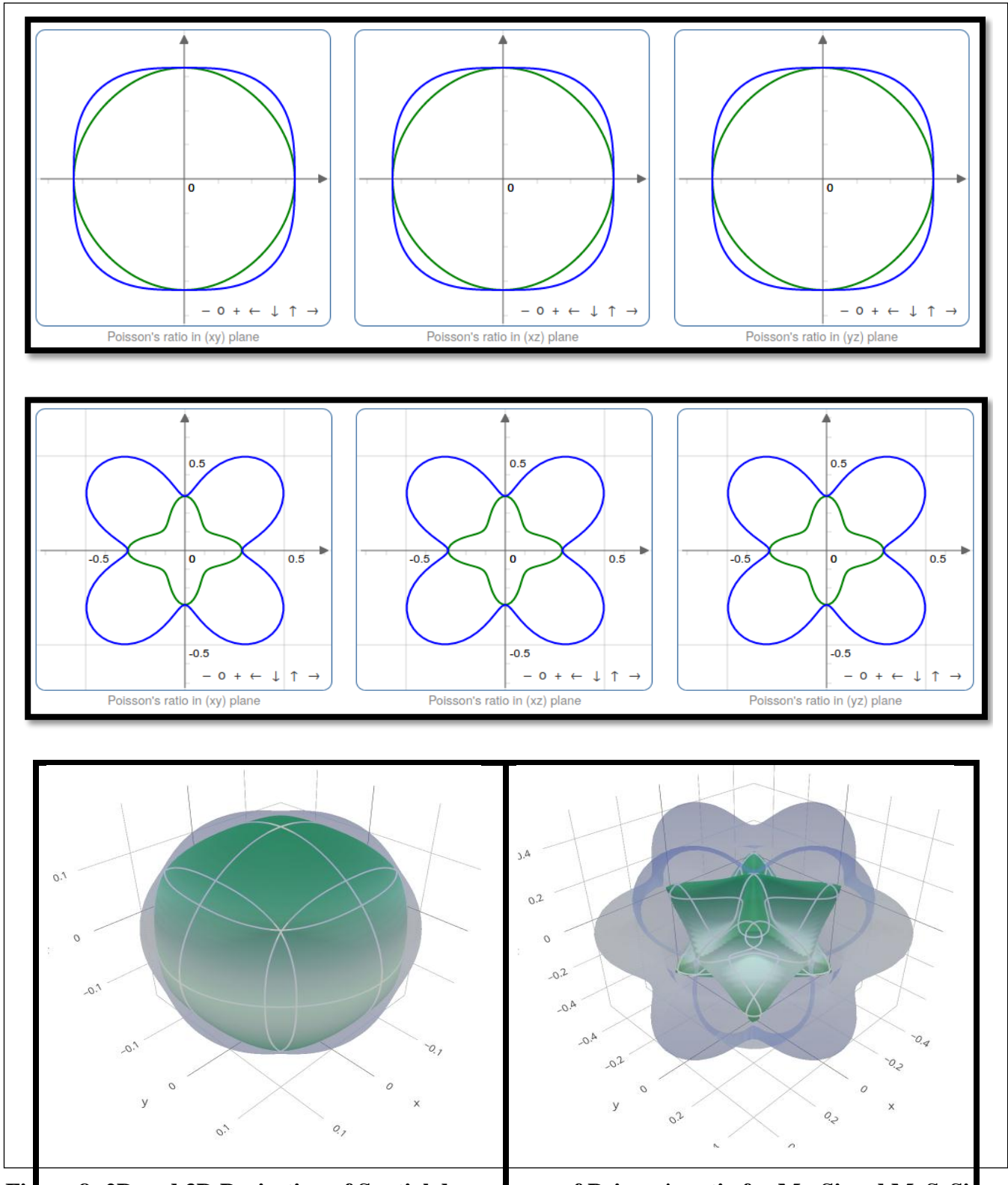


Figure 8: 2D and 3D Projection of Spatial dependence of Poisson's ratio for Mg₂Si and MgSiSi

4. Conclusion

The elastic and thermal properties of metallic alloys are important characteristics that inform as well as direct their applicability in the design of modern projects ranging from photonics to thermionics, to production of cutting tools and automobile parts. Owing to the foregoing this study evaluated by way of computational modeling the elastic and thermal properties of $MgXSi$ ($X=Mg, Sr$) compounds employing the projector augmented wave (PAW) variant of pseudo-potential plane-waves approach, for the exchange and correlation potential. Elastic constants and elastic compliances of $MgXSi$ as well as the vibrational free energies, entropy, constant volume specific heat capacities were computed. This study recorded anelastic constant, C_{11} of 166.8GPa at the Debye temperature of 341.9K for $MgSrSi$. At 300K, the constant volume specific heat capacity, C_v for Mg_2Si and $MgSrSi$ were 62.8 J/K/(N mol) and 70 J/K/(N mol) respectively. From the results, it is concluded that the elastic constants of Mg_2Si is quite consistent with theoretical results already recorded on the subject and compares favourably with experimental data. It is submitted that the elastic and thermodynamic of $MgXSi$ ($X=Mg, Sr$) has been successfully computed. Thus, It may be concluded that at a fixed volume, the thermodynamic or heat capacity of $MgXS$ rises with temperature even at low temperatures.

ACKNOWLEDGEMENT

A Eulogy to an Eminent Professor: Prof. John O.A. Idiodi

Unarguably some scholars are born and some are made. Permit me to rightly accord the 'born' perspective to my erudite scholar and mentor who I could unequivocally attest to the fact that my meeting with him in 2011 marked the beginning of my odyssey to fulfilling my life's destiny as ordained by God.

Our beloved Prof! You are not just a scholar for there are millions of scholars the world over, but you have unambiguously and meritoriously distinguished yourself from the millions of scholars. You have proved that a scholar can be a true mentor, a father, an advocate, a friend, confidant, and a colleague all at the same time. You are indeed a rare gem and posterity will ever attest to the positive influence you enshrined on the hearts and future of many of us who were opportune to pass through your mentorship.

Our Dear Professor, you will always remain revered and evergreen in our heart of hearts. You came! You saw! You conquered and won. Your meritorious and untainted service shall ever glow beyond the academic skies. We are convinced you are not tired, but as the chapter 3 and verse number 1 of the bible book of Ecclesiastes rightly averred: "To everything there is a season, and a time to every purpose under heaven..." Your service to humankind has outlasted many seasons but my Prof, it is our belief that your retirement from active service is a substantive evidence that cannot be controverted anywhere.

My Prof. I cannot possibly fathom all that you did but our collective prayer for you is this: May the good Lord bless you, strengthen you, cause his face to shine upon you, and add to you many more happier years in Jesus name. Amen.— Dr. A.S. Olayinka

REFERENCES

- [1] Liu Na-Na, Song Ren-Bo, and Du Da-Wei (2009). Elastic constants and thermodynamic properties of $Mg_2Si_{1-x}Sn_x$ from first-principles calculations. Chinese Journal of Physics, 18(5), pp. 1674-1056
- [2] Schulz T, Ruffel M. and Pixius K.(1999) Powder Technology, 105, 149
- [3] Noda Y, Otsuka N and Matsumoto K.(1989). Journal of Applied Physics, pp.53 487
- [4] Zhang Junqin, Huihui Ma, Bin Zhao, Qun Wei and Yintang Yang (2018). Electronic and Elastic properties of the antiferroelectric structure Mg_2Si under pressure. AIP Conference Proceedings 1971, 020018; <https://doi.org/10.1063/1.5041113>
- [5] Li S B, Li X N, Dong C, Jiang X.(2010) Acta Phys.Sin.59 4267(in Chinese)
- [6] Saravanan R, Robert M. C.(2009) J. Alloys Compd.47926

- [7] Olayinka, A.S., Adetunji, B.I., Idiodi, J.O.A. and Aghemelon, U. (2019) Ab initio study of electronic and optical properties of nitrogen-doped rutile TiO₂. *International Journal of Modern Physics B*, 33(6), 1950036. <https://doi.org/10.1142/S021797921950036X>
- [8] Olayinka A. S., Nwankwo W. & Idiodi J. O. A. (2019). Electronics and Optical Properties of Nitrogen Doped Anatase for Solar Application. *Covenant Journal of Physical & Life Sciences*, 7(2)
- [9] Adetunji B.I., **Olayinka A.S.**, Fashae, J.B., Ozebo V.C. and Adebayo G.A. (2016) Ab-initio investigation of the electronic, lattice dynamic and thermodynamic properties of ScCd intermetallic alloy. *International Journal of Modern Physics B*, 30(24), 1650175. DOI: 10.1142/S0217979216501757
- [10] Hao J, Zou B, Zhu P, Cao C, Li Y, Liu D, Wang K, Lei W, Cui Q, Zou G.(2009) *Solid State Commun.* 149 689
- [11] W. Kohn, L.J. Sham, *Phys. Rev.* 140 (1965) 1133.
- [12] Monkhorst, H. J. & Pack, J. D.(1976). Special points for Brillouin-zone integrations. *Phys. Rev. B*, 13, pp. 5188-5192.
- [13] Fletcher, R.(1987). *Practical Methods of Optimization* (2nd ed). New York: John Wiley & Sons. https://dalcorso.github.io/thermo_pw/
- [14] Giannozzi P., Baroni S., Bonini N., Calandra M., Car, R., Cavazzoni C., Ceresoli D., Chiarotti G. L., Cococcioni M., Dabo I., Dal Corso A., Fabris S., Fratesi, G., de Gironcoli S., Gebauer R., Gerstmann U., Gougoussis C., Kokalj A., Lazzeri M., Martin-Samos L., Marzari N., Mauri F., Mazzarello R., Paolini S., Pasquarello A., Paulatto L., Sbraccia C., Scandolo S., Sclauzero G., Seitsonen A. P., Smogunov A., Umari P. and Wentzcovitch R. M.(2009). QUANTUM ESPRESSO: a modular and open-source software project for quantum simulations of materials. *J. Phys.: Condens. Matter* 21, p. 395502
- [15] Giannozzi, P Andreussi, O Brumme, T Bunau, O Buongiorno Nardelli, M Calandra, Car, R Cavazzoni, C Ceresoli, D Cococcioni, M Colonna, N Carnimeo, I Dal Corso, A de Gironcoli, S Delugas, P DiStasio, R A Ferretti, A Floris, A Fratesi, G Fugallo, G Gebauer, R Gerstmann, U Giustino, F Gorni, T Jia, J Kawamura, M Ko, H-Y Kokalj, A Küçükbenli, E Lazzeri, M Marsili, M Marzari, N Mauri, F Nguyen, N L Nguyen, H-V Otero-de-la-Roza, A Paulatto, L Poncé, S Rocca, D Sabatini, R Santra, B Schlipf, M Seitsonen, A P Smogunov, A Timrov, I Thonhauser, T Umari, P Vast, N Wu, X Baroni, S (2017). Advanced capabilities for materials modelling with Quantum ESPRESSO. *Journal of Physics: Condensed Matter*, 29 (46) 465901.
- [16] Gaillac R., Pullumbi P. and Coudert F. (2016). ELATE: an open-source online application for analysis and visualization of elastic tensors. *Journal of Physics: Condensed Matter*, 28(27). 275201. 10.1088/0953-8984/28/27/275201
- [17] Olayinka A. S., Odeyemi E. O. and Okwunjor, O. Phonon Dispersion and Thermodynamic Properties of Ytterbium. (2016). *BIU Journal of Basic and Applied Sciences*, 2(1), pp. 84-93.
- [18] Eryigit, T. & Gurel, R., 2010. Ab initio lattice dynamics and thermodynamics of rare-earth hexaborides LaB₆ and CeB₆. *Phys. Rev. B*, Vol. 82, p. 104302-12.
- [19] Debye, P.(1912). Zur Theorie der spezifischen Wärmen. *Ann. Phys.*, 39, pp. 789-839.
- [20] Wang, R.; Wang, S.; Wu, X.; Lan, M.; & Song, T.(2012). First-principles calculations of phonon and thermodynamic properties of AIRE (RE = Y, Gd, Pr, Yb) intermetallic compounds. *Phys. Scr.*, 85, p. 035705-1-8.
- [21] Siegfried Haussühl (2003). *Microscopic and Macroscopic Properties of Solids. Assessment of Safety and Risk with a Microscopic Model of Detonation*, pp.493-554.
- [22] Madelung, O. and Ornstein, L. B.(1983). *Numerical Data and Functional Relationships in Science and Technology*, New Series, Group III, 17e, Springer-Verlag, Berlin, pp.163-432.

- [23] Robert D. Schmidt, Eldon D. Case, Jesse Giles, Jennifer E. Ni, and Timothy P. Hogan (2012) Room-Temperature Mechanical Properties and Slow Crack Growth Behavior of Mg₂Si Thermoelectric Materials. *Journal of Electronic Materials*, 41(6), pp.1210 – 1216. DOI: 10.1007/s11664-011-1879-3
- [24] Yu, B., Chen, D., Tang, O., Wang, C. and Shi D. (2010). Structural, electronic, elastic and thermal properties of Mg₂Si. *Journal of Physics and Chemistry of Solids*, 71, pp. 58–763
- [25] Romain Gaillac, Pluton Pullumbi and François-Xavier Coudert(2016). ELATE: an open-source online application for analysis and visualization of elastic tensors.*Journal of Physics: Condensed Matter*, 28(27),275201. 10.1088/0953-8984/28/27/275201